Original article

Silver nanoparticles inhibit hepatitis B virus replication

Lei Lu[1†], Raymond Wai-Yin Sun[2†], Rong Chen[2], Chee-Kin Hui[3], Chi-Ming Ho[2], John M Luk[4], George KK Lau[1]* and Chi-Ming Che[2]*

[1]Department of Medicine, The University of Hong Kong, Pokfulam Road, Hong Kong, China
[2]Department of Chemistry and Open Laboratory of Chemical Biology of the Institute of Molecular Technology for Drug Discovery and Synthesis, The University of Hong Kong, Pokfulam Road, Hong Kong, China
[3]Department of Microbiology, The University of Hong Kong, Pokfulam Road, Hong Kong, China
[4]Department of Surgery, The University of Hong Kong, Pokfulam Road, Hong Kong, China

[†]These authors made an equal contribution to this work
*Corresponding authors: E-mail: cmche@hku.hk; E-mail: gkklau@netvigator.com

Background: Silver nanoparticles have been shown to exhibit promising cytoprotective activities towards HIV-infected T-cells; however, the effects of these nanoparticles towards other kinds of viruses remain largely unexplored. The aim of the present study was to investigate the effects of silver nanoparticles on hepatitis B virus (HBV).

Methods: Monodisperse silver nanoparticles with mean particle diameters of ~10 nm (Ag10Ns) and ~50 nm (Ag50Ns) were prepared from $AgNO_3$ in HEPES buffer. The *in vitro* anti-HBV activities of these particles were determined using the HepAD38 cell line as infection model.

Results: Ag10Ns and Ag50Ns were able to reduce the extracellular HBV DNA formation of HepAD38 cells by >50% compared with the vehicle control (that is, HepAD38 cells in the absence of silver nanoparticles). Silver nanoparticles had little effect on the amount of HBV covalently closed circular DNA (cccDNA), but could inhibit the formation of intracellular HBV RNA. Gel mobility shift assays indicated that Ag10Ns bound HBV double-stranded DNA at a DNA:silver molar ratio of 1:50; an absorption titration assay showed that the nanoparticles have good binding affinity for HBV DNA with a binding constant (K_b) of $(8.8 \pm 1.0) \times 10^5$ dm^3mol^{-1}. As both the viral and Ag10Ns systems are in the nanometer size range, we found that Ag10Ns could directly interact with the HBV viral particles as revealed by transmission electronic microscopy.

Conclusions: Silver nanoparticles could inhibit the *in vitro* production of HBV RNA and extracellular virions. We hypothesize that the direct interaction between these nanoparticles and HBV double-stranded DNA or viral particles is responsible for their antiviral mechanism.

Introduction

Hepatitis B virus (HBV) is a partially double-stranded (ds) DNA virus that chronically infects more than 400 million people worldwide. The persistence of HBV is associated with the development of liver cirrhosis and hepatocellular carcinoma [1,2]. After the entry of HBV virions into the hepatocyte, viral core particles migrate to the nucleus where the viral genome is repaired to form a covalently closed circular DNA (cccDNA) that forms the template for the transcription of viral messenger RNA (mRNA) and 3.5 kb pregenomic RNA (pgRNA) [3,4]. The pgRNA serves as the template for the reverse transcription and for the synthesis of viral genomes [5]; thus, the transcription of pgRNA from cccDNA is a key event in HBV replication.

By 2007, six agents were registered for the treatment of chronic HBV infection. Two are immunomodulatory agents, namely conventional interferon (IFN)-α2b and pegylated IFN-α2a, which aim to restore host immune control on HBV and thus lead to sustained off-treatment disease remission. The other four agents are nucleos(t)ide analogues (lamivudine, adefovir, entecavir and telbuvidine) with direct antiviral activity [6]. IFN-α can promote the lysis of infected hepatocytes by both CD8^{+} cytotoxic T-lymphocytes and natural killer cells [7]; moreover, IFN-α can directly inhibit the synthesis of viral proteins by modulating the action of antiviral cytokines [8]. However, the use of IFN-α is hampered by the serious side effects and low success

rates [9]. Nucleos(t)ide analogues act mainly as specific inhibitors of the viral polymerase reverse transcriptase. Although the treatment of chronic hepatitis B (CHB) with nucleos(t)ide analogues produces rapid suppression of HBV replication in the short-term, this effect is not often sustainable due to the emergence of drug-resistant HBV strains [10]. It is therefore important to develop new antiviral strategies to combat wild-type and mutant HBV infections.

Although the use of metal nanoparticles in catalysis and optoelectronic devices has been extensively investigated [11–13], there have been relatively few studies on their biological properties and potential therapeutic applications [14,15]. In this regard, the antimicrobial activities of silver nanoparticles have received the most attention [16,17], and proteomic and biochemical studies on the antibacterial and/or fungal activities of silver nanoparticles have been reported [16]. In the literature, there are only two published studies on the antiviral activities of silver nanoparticles: both reporting their anti-HIV-1 properties [18,19]. It was found that silver nanoparticles could bind to HIV viral particles with a regular spatial arrangement and were able to inhibit the virus from binding to host cells [18]. Also, silver nanoparticles can inhibit the replication of HIV and exhibit promising cytoprotective activities toward HIV-infected T-cells [19]. Indeed, studies on the interaction of metal nanoparticles with viruses are sparse [18–20], despite both systems falling in the nanometer range.

In this study, we prepared monodisperse silver nanoparticles with mean particle diameters of ~10 nm (Ag10Ns) and ~50 nm (Ag50Ns) from $AgNO_3$ in 4-(2-hydroxyethyl)-1-piperazineethanesulfonic acid (HEPES) buffer. The *in vitro* anti-HBV activities of these particles were determined using the HepAD38 cellular model [21]. We found that silver nanoparticles could interact with HBV dsDNA and viral particles, and were able to inhibit the *in vitro* production of HBV RNA and extracellular virions.

Methods

Preparation and characterization of silver nanoparticles

Ag10Ns (~10 nm) silver particles were prepared by adding $AgNO_3$ solution (1 ml, 50 mM) to a HEPES buffer (48 ml, 10 mM, pH 7.4). The mixture was then refluxed for 2 h with vigorous stirring. A resultant golden yellow solution with a surface plasmon resonance (SPR) absorption peak at ~400 nm was obtained, revealing the formation of silver nanoparticles. Likewise, Ag50Ns (~50 nm) particles were obtained by adding $AgNO_3$ (1 ml, 50 mM) solution and sodium citrate (0.01 g) to a HEPES buffer (48 ml, 10 mM, pH 7.4). The mixture was heated under reflux for 2 h and a resultant golden yellow solution with an SPR absorption peak at ~400 nm was obtained, revealing the formation of silver nanoparticles. Ag800Ns (~800 nm) were prepared by adding $AgNO_3$ (1 ml, 50 mM) solution and ascorbic acid (0.05 g) to a HEPES buffer (48 ml, 10 mM, pH 7.4). After stirring for 10 min, the mixture was heated at 40°C with stirring for 2 h. Silver nanoparticles (Ag800Ns) were obtained.

The X-ray diffraction (XRD) spectra of silver nanoparticles were recorded with a Philips PW1830 powder X-Ray diffractometer (Phillips, Madrid, Spain). The UV-vis absorption spectra were recorded using a Perkin-Elmer Lambda 900 UV-vis spectrophotometer (Perkin-Elmer, MA, USA). Transmission electronic microscopy (TEM) images of the silver nanoparticles were obtained with JEOL JEM-2000 transmission electromicroscopy (accelerating voltage of 200 kV), Philips Tecnai 20 equipped with Oxford incax-sight EDX attachment (accelerating voltage of 200 kV) or Philips EM208s (accelerating voltage of 80 kV).

Stability evaluation

The UV-vis absorption spectra of both Ag10Ns and Ag50Ns in aqueous solution were monitored over 48 h and 3 months. Their stabilities in physiologically relevant medium (HEPES buffer, pH 7.4) were also monitored by UV-vis spectrophotometry.

Cell culture

The HepAD38 cell line was maintained in Dulbecco's modified Eagle's medium (Invitrogen, CA, USA) supplemented with fetal bovine serum (10% v/v), L-glutamine (2 mM), penicillin (50 µg/ml), streptomycin (100 µg/ml), kanamycin (50 µg/ml), geneticin (400 µg/ml) and tetracycline (0.3 µg/ml). Cells were incubated at 37°C in a 5% CO_2 humidified atmosphere.

Antiviral and cytotoxicity assays

To assess the antiviral activity of silver nanoparticles, HepAD38 cells were seeded into 24-well microtitre plates (2×10^5 cells/well) and grown for 3 days in the presence of tetracycline (0.3 µg/ml). The cells were washed twice with phosphate-buffered saline (PBS) and treated with tetracycline-free medium that contained either a test or control compound. The cell cultures were incubated at 37°C in a 5% CO_2 humidified atmosphere for 48–96 h. The cell medium was then collected and total DNA was extracted from the medium using the QIAamp DNA Blood Mini Kit (QIAGEN, Hilden, Germany). A quantitative real-time polymerase chain reaction (PCR) assay for the detection of HBV DNA was performed as described previously [22].

To assess the cytotoxic effects of silver nanoparticles, HepAD38 cells were seeded into 96-well plates at a density of 2×10^4 cells/well and exposed to silver nanoparticles with a treatment schedule identical to that described above for the antiviral assays. Following drug treatment, cell viability was assessed by a modified method of the Mosmann-based 3-(4,5-dimethylthiazol-2-yl)-2,5-diphenyltetrazolium bromide (MTT) assay [23].

HBV RNA and cccDNA detection

HepAD38 cells were seeded into 24-well microtitre plates (2×10^5 cells/well) and grown for 3 days in the presence of tetracycline (0.3 µg/ml). The cells were washed twice with PBS and treated with tetracycline-free medium with or without Ag10Ns (1–10 µM). The cell cultures were incubated at 37°C in a 5% CO_2 humidified atmosphere for 24, 48, 72 or 96 h. At the end of the incubation, adhesive HepAD38 cells were trypsinized, washed with PBS and divided into two aliquots for DNA extraction and RNA extraction. Total cellular DNA was extracted using the QIAamp DNA Blood Mini Kit (QIAGEN), and used for HBV cccDNA quantification by real-time PCR as described [24]. Total RNA was extracted from the cells using the RNAeasy Mini Kit (QIAGEN); HBV RNA was detected by real-time reverse transcription PCR (RT-PCR) with the TaqMan One-Step RT-PCR Master Mix Reagents (Applied Biosystems, CA, USA) according to the manufacturer's instructions, using the 5′ HCF primer (5′-GTGTCTTTTGGAGTGTG-GATTCG nt2258–2280) and 3′ antisense HCR primer (5′-TCGTCGTCTAACAACAGTAGTTTCC nt2356–2332). The house-keeping gene glyceraldehyde-3-phosphate dehydrogenase (GAPDH) was used as an endogenous control to normalize the quantity of total human RNA in the template, and the Human GAPDH Endogenous Control™ (VIC/TAMRA Probe, Primer Limited, Applied Biosystems) was used for GAPDH mRNA amplification and detection. The relative quantity of HBV RNA was calculated through comparison with the quantity of GAPDH by $2^{-\Delta\Delta CT}$ method [25].

Cellular uptake experiments

Cellular uptake experiments were conducted according to the method described in the literature [26] with some modifications. HepAD38 cells (2×10^5 cells/well) were seeded in 24-well plates with culture medium (1 ml/well) and incubated at 37°C in an atmosphere of 5% CO_2 for 24 h. The culture medium was removed and replaced with medium containing silver nanoparticles at a concentration of 5 µM. After exposure to the silver nanoparticles for 2, 4 and 24 h, the medium was removed and the cell monolayer was washed four times with ice-cold PBS. Milli-Q water (1 ml) was added and the cell monolayer was scraped off the well. Samples (300 µl) were digested in 70% HNO_3 (500 µl) at 70°C for 2 h then diluted 1:100 in water for analysis by inductively coupled plasma mass spectrometry (ICP-MS).

Gel mobility shift assay

Full-length HBV dsDNA was produced according to a previously described method [27]. HBV dsDNA treated with Ag10Ns at different molar ratios (dsDNA:Ag10Ns 1:50, 1:5, 1:0.5 and 1:005) as well as the vehicle control (that is, HepAD38 cells in the absence of silver nanoparticles) were resolved by 3% agarose gel electrophoresis.

Absorption titration

A solution of the silver nanoparticles in PBS (95% v/v) was placed in a thermostatic cuvette in a UV-vis spectrometer and an absorption spectrum recorded. Aliquots of a millimolar stock DNA solution were added to the solution of silver nanoparticles and absorption spectra were recorded after equilibration for 10 min per aliquot until saturation point was reached. The binding constant K_b can be determined from the following equation:

$$[DNA]/\Delta\varepsilon_{ap}=[DNA]/\Delta\varepsilon+1/(\Delta\varepsilon+K_b),$$

where $\Delta\varepsilon_{ap}=|e_A-e_B|$ in which e_A is the A_{obs}/[silver nanoparticles] and $\Delta\varepsilon=|e_B-e_F|$ with e_B and e_F corresponding to the extinction coefficients of the DNA-bound and unbound silver nanoparticles, respectively [28]. A plot of $[DNA]/\Delta\varepsilon_{ap}$ versus $[DNA]$ will have a slope of $1/\Delta\varepsilon$ and a y intercept equal to $1/(\Delta\varepsilon K_b)$. K_b is given by the ratio of the slope to the y intercept.

Measuring the interaction between silver nanoparticles and HBV virions

Ag10Ns were coated on the surface of 96-well plates and serum samples of CHB patients, containing 1×10^7 HBV virions/ml, were incubated in treated or untreated (control) wells for 0–60 min. At 10 min intervals, the serum samples in the treated and control wells were collected and subjected to quantitative PCR following total DNA extraction.

Electron microscopy

HepAD38 cells were treated with Ag10Ns (5 µM) for 96 h at 37°C and were pelleted in a 1.5 ml centrifuge tube at 2,000 rpm for 10 min. Supernatant was removed and the cell pellet fixed in glutaraldehyde (2.5%) for 12 h at 4°C. The pellet was then washed three times in PBS, and incubated in OsO_4 (2%) and $K_3Fe(CN)_6$ (1%) for 1 h. After three further PBS

washes, pellets were dehydrated and infiltrated in a 1:1 mixture of propylene oxide and embedded in resin. Ultrathin (50 nm) sections were collected on 200-mesh copper grids and stained with uranyl acetate (6%) in double-distilled water for 10 min followed by lead citrate (1%) for 15 min. Sections were viewed using a Philips EM208s transmission electron microscope at 80 kV.

Results and discussion

Characterization and stability of silver nanoparticles

In this work, we prepared monodisperse silver nanoparticles with mean particle diameters of ~10 nm (Ag10Ns), ~50 nm (Ag50Ns) and ~800 nm

(Ag800Ns) from $AgNO_3$ in HEPEs buffer. The silver nanoparticles were characterized by TEM (Supplementary material; Figure S1), X-ray powder diffraction (XRD; Figure S2) and energy dispersive X-ray analysis (EDX; Figure S3).

The silver nanoparticles Ag10Ns and Ag50Ns were found to be stable in water, with no significant spectral changes observed over a 48 h period at 37°C based on UV-vis spectrophotometric measurements. In contrast, although we did not detect any spectral changes for solutions of Ag800Ns within the first few hours, after incubation at 37°C for 48 h there was an approximate 38% decrease in absorbance at the λ_{max} (Figure S3). Previously, human serum albumin (HSA) was reported to stabilize silver nanoparticles. In this work, we found

Figure 1. The antiviral effects and cytotoxicity of silver nanoparticles
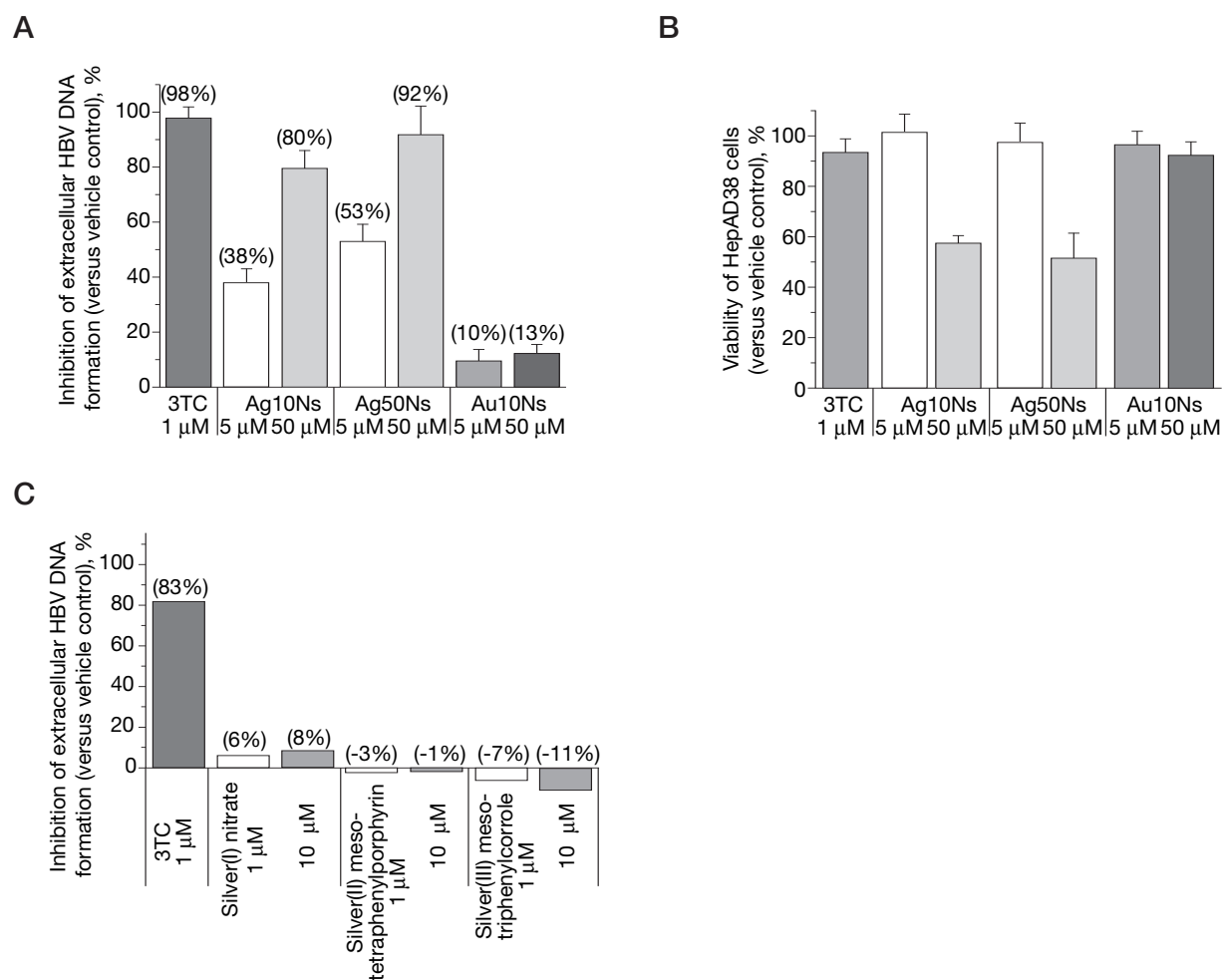
(A) Percentage inhibition (versus vehicle control) of extracellular hepatitis B virus (HBV) formation in HepAD38 cells (48 h) by silver (Ag10Ns and Ag50Ns) and gold (Au10Ns) nanoparticles. **(B)** Cell viability of HepAD38 cells in the presence of silver (Ag10Ns and Ag50Ns) and gold (Au10Ns) nanoparticles. **(C)** Percentage inhibition (versus vehicle control) of extracellular HBV formation in HepAD38 cells (48 h) by silver compounds with silver in different oxidation states, including $Ag^I NO_3$, $[Ag^{II}(TPP)]$ ($H_2TPP=$*meso*-tetraphenylporphyrin) and $[Ag^{III}(TPC)]$ ($H_3TPC=$*meso*-triphenylcorrole). The antiviral effect of the known anti-HBV drug lamivudine (3TC) is also included for comparison. **(D,E,F,G)** Dose-dependent anti-HBV and cytotoxic effects of Ag10Ns at **(D,F)** t=48 and **(E,G)** t=96 h.

that HSA was able to stabilize silver nanoparticles Ag10Ns and Ag50Ns, with no significant UV-vis spectral changes observed over a 3-month period.

Antiviral effects and cytotoxicity of silver nanoparticles

HepAD38 is a stably transfected hepatoblastoma cell line that secretes HBV-like particles and expresses high levels of HBV DNA into its surrounding medium (supernatant) [21]. To test the anti-HBV activity of silver nanoparticles, HepAD38 cells were separately treated with silver nanoparticles Ag10Ns and Ag50Ns at concentrations of 5–50 µM. After 48 h incubation, total DNA was extracted from the supernatants, and the HBV DNA levels were quantified by quantitative real-time PCR. Parallel cytotoxicity evaluation was done by MTT assay [23]. Compared with the drug-free vehicle control, both Ag10Ns and Ag50Ns were found to exhibit potent anti-HBV activities (Ag10Ns showed 38% inhibition at 5 µM and 80% at 50 µM; Ag50Ns showed 53% inhibition at 5 µM and 92% at 50 µM); the results are depicted in Figure 1A. Over 90% cell viability was observed for Ag10Ns and Ag50Ns at

5 µM (Figure 1B). In contrast, the viability of HepAD38 cells decreased in the presence of silver nanoparticles at a concentration of 50 µM for both Ag10Ns and Ag50Ns. The induced cytotoxicity could be accounted for by the aggregation of silver nanoparticles at high concentrations. Silver nanoparticles (Ag800Ns) with particle diameters of 800 nm were found to induce severe cytotoxicity to the HepAD38 cells even at the 5 µM level; thus, their potential anti-HBV activity was not examined. For comparison, gold nanoparticles (10 nm, Au10Ns) prepared by sodium citrate reduction were found to exhibit relatively low anti-HBV activity (10–13%). Silver compounds with silver in different oxidation states, including $Ag^{I}NO_3$, $[Ag^{II}(TPP)]$ ($H_2TPP=meso$-tetraphenylporphyrin) and $[Ag^{III}(TPC)]$ ($H_3TPC=meso$-triphenylcorrole), also showed no significant anti-HBV activities (Figure 1C). Taken together, the results indicate that the anti-HBV effects of silver nanoparticles are significant when compared with gold nanoparticles and other classes of silver complex.

Using Ag10Ns as an example, the dose-dependent (from 0.1 to 50 µM) anti-HBV effects of silver
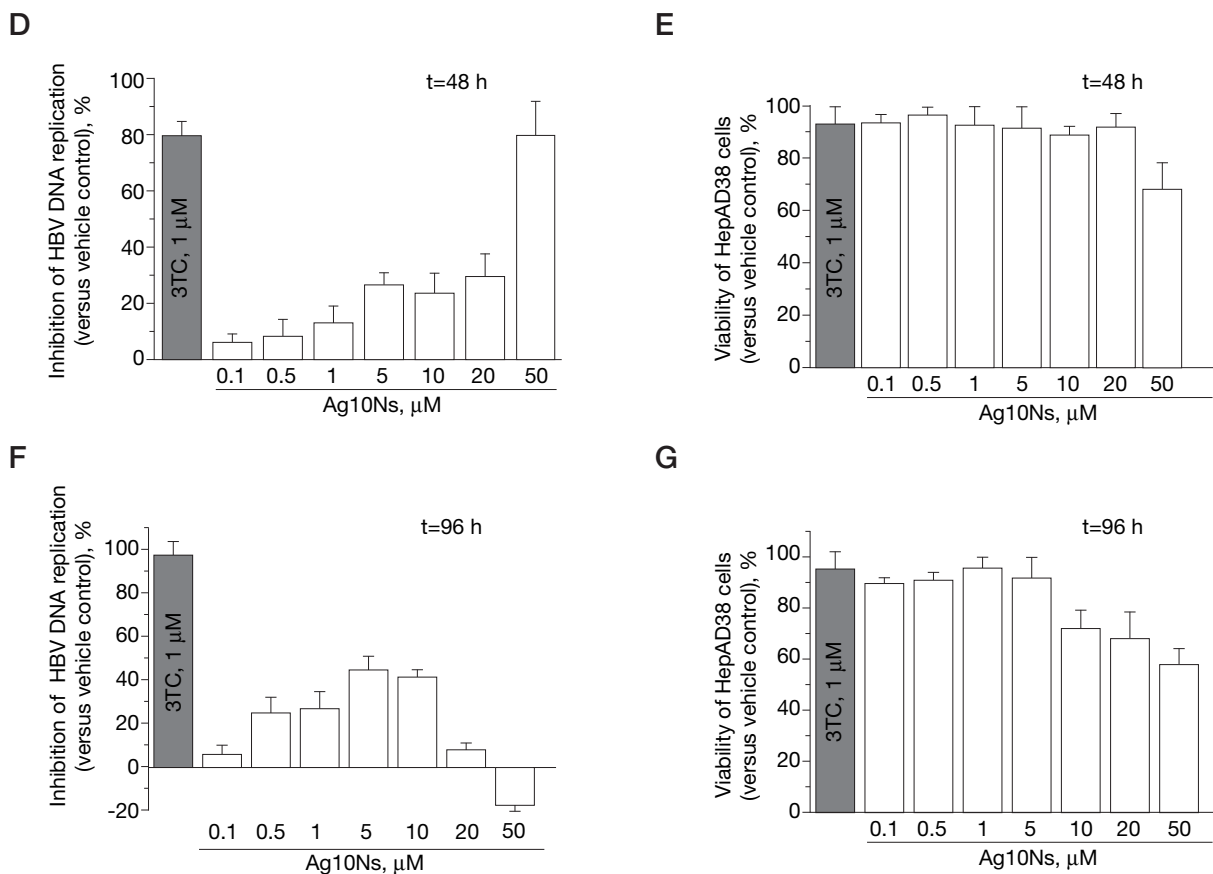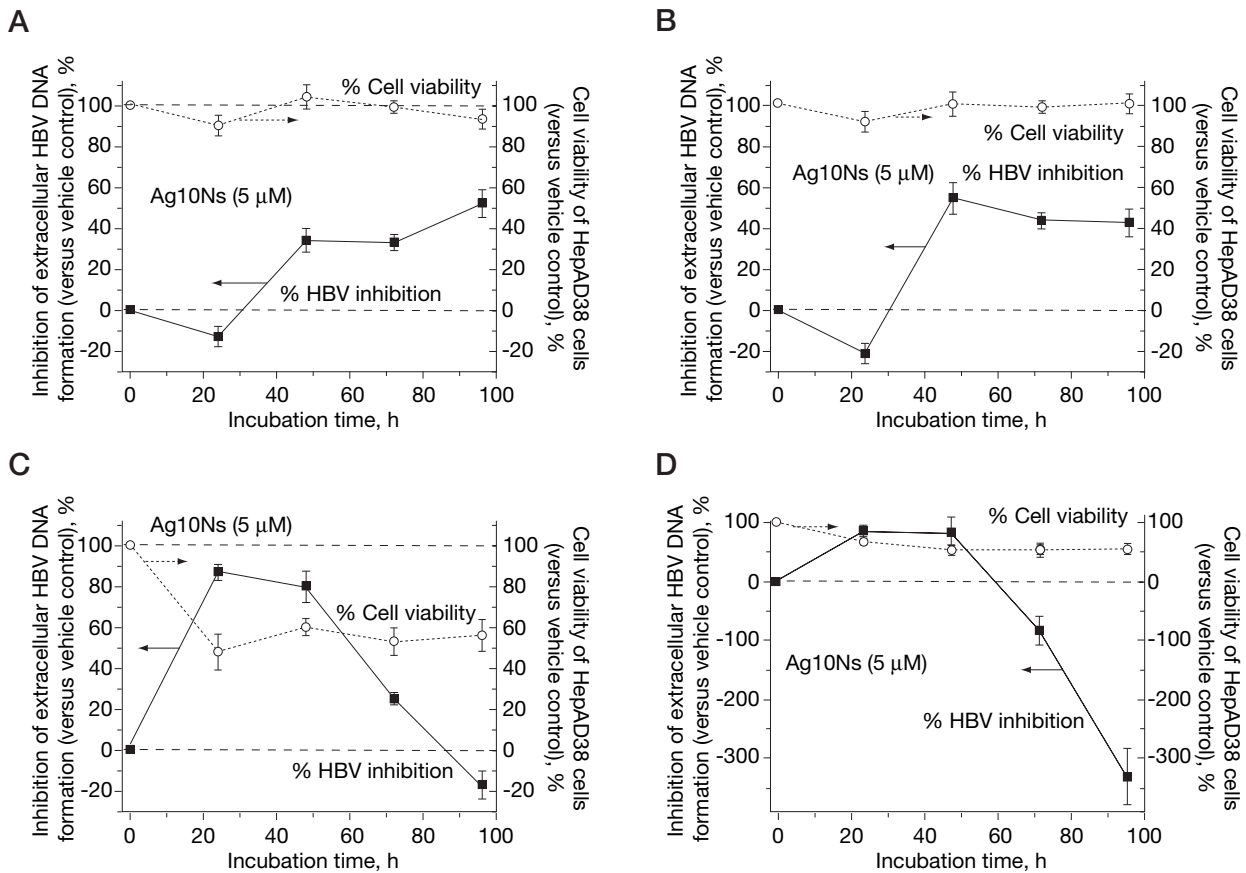

Figure 1. Continued

Figure 2. The time-dependent anti-HBV activity of silver nanoparticles

Percentage hepatitis B virus (HBV) inhibition (y axis, left; solid line) and cell viability (y axis, right; dotted line) of HepAD38 cells versus vehicle control with increasing incubation times (0–96 h). Arrows indicate which axis should be referred to. Horizontal dashed lines represent the baselines. **(A)** 5 µM Ag10Ns, **(B)** 5 µM Ag50Ns, **(C)** 50 µM Ag10Ns, **(D)** 50 µM Ag50Ns.

nanoparticles were examined. Compared with the vehicle control, Ag10Ns inhibit HBV DNA replication in a dose-dependent manner after 48 h incubation (Figure 1D). However, Ag10Ns was found to achieve maximum inhibitory effect at a concentration of 5 µM with prolonged incubation (96 h), whereas the anti-HBV effect was reduced or reversed at higher concentrations (10, 20 and 50 µM; Figure 1F). The plateau effect of the antiviral activity could be explained by the release of intracellular HBV DNA at high concentrations of Ag10Ns. As mentioned, treatments of Ag10Ns at high concentrations were cytotoxic to the host HepAD38 cells (Figure 1E,G) and the intracellular HBV DNA might be released from the lysed cells. Prolonged incubation with high dosages of silver nanoparticles could have led to the sustained release of intracellular DNA to the surroundings and counteracted the antiviral effects of the silver nanoparticles.

The time-dependent anti-HBV activities of silver nanoparticles were further examined at various time points from 0 to 96 h. In this study, supernatants of HepAD38 cells were collected (0, 24, 48, 72 and 96 h) after the introduction of Ag10Ns. The time dependence of the percentage inhibition of extracellular HBV DNA production by Ag10Ns at a concentration of 5 µM level was first examined, with the results plotted in Figure 2A (solid line). Ag10Ns exhibited ~30% inhibition at t=48 and 72 h, and achieved over 50% inhibition at t=96 h. Notably, parallel MTT assays revealed that >95% of the Ag10Ns-treated cells remained viable (Figure 2A, dotted line). Similar to Ag10Ns, Ag50Ns at 5 µM also inhibited HBV replication (~50% at t=48, 72 and 96 h; Figure 2B, solid line), with over 95% viable cells detected (dotted line). At a concentration of 50 µM, both Ag10Ns and Ag50Ns exhibited potent inhibitory activities of extracellular HBV formation at 24 or 48 h of incubation (solid lines, Figures 2C and 2D, respectively). After these time points, the sustaining cytotoxic effects (dotted lines, Figures 2C and 2D, respectively) enhanced the release of intracellular HBV DNA to the surroundings.

To determine whether or not binding to HSA would alter their biological activities, the anti-HBV activities of the silver nanoparticles were examined after incubation with HSA at a concentration 2 mM. Similar levels of potency were observed for both the HSA-free and HSA-bound nanoparticles (for example, 41% and 73% at 5 and 50 µM of HSA-Ag10Ns, respectively). This result suggests that HSA might also serve as a carrier for the silver nanoparticles to the biological targets, that is, HBV-infected cells.

Uptake of silver nanoparticles and effects on the HBV life cycle

The uptake of silver nanoparticles by HepAD38 cells was examined. After treatment with Ag10Ns (5 µM, 2 h incubation), the cells were collected and subjected to ICP-MS to analyse the silver content. Cell-free samples (100% silver content) were compared with cells treated with Ag10Ns absorbed (~15% of silver). The high level of initial cellular uptake implied that some silver nanoparticles could reach their potential intracellular target(s) (for example, HBV DNA, RNA and cccDNA, etc) by passing through the membranes of HepAD38 cells.

Using Ag10Ns as the model, the HBV replicative intermediates were examined at various time points in order to elucidate the effects of silver nanoparticles on the HBV life cycle. HepAD38 cells were treated with Ag10Ns at 5 µM for 0, 24, 48, 72 and 96 h. At each time point, the cells were collected and the total DNA and RNA were extracted. The HBV pgRNA and precore/core promoter directed RNA were relatively quantified through one step quantitative real-time PCR, and GAPDH was used as an endogenous control to normalize the quantity of total cellular RNA in the template. We found that Ag10Ns could inhibit the production of HBV RNA in a dose-dependent manner (Figure 3), and the percentage inhibition at 10 µM increased from 44.6% at 24 h to 67.9% at 48 h, reaching a peak of 72.5% at 72 h. After this time, inhibition dropped to 46.3% at 96 h. HBV covalently closed circular DNA (cccDNA) levels were also quantified according to a previously described method [24]. However, no significant difference was observed between the cccDNA levels in treated HepAD38 cells and in the vehicle control at various time points (0 to 96 h; data not shown).

Silver nanoparticles had little effect on the cccDNA levels, but could inhibit the formation of HBV RNA. The reduction of HBV RNA levels suggested that transcription from the cccDNA or integrated HBV genome was impeded, which could result in the inhibition of HBV relaxed circular DNA (rcDNA) formation because pgRNA serves as the template of the reverse transcription. Most of the rcDNA is packaged into core particles and exported from the cells, whereas only a few cores need to be transported back to the nucleus

Figure 3. The inhibition of HBV RNA production by Ag10Ns
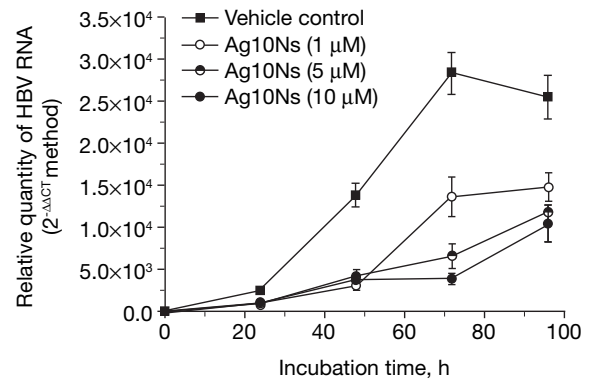
Relative quantification of hepatitis B virus (HBV) RNA (calculated by the comparative $2^{-\Delta\Delta CT}$ method) in Ag10Ns-treated (1–10 µM) HepAD38 cells and a drug-free vehicle control with incubation times of 0, 24, 48, 72 and 96 h.

where rcDNA is converted to cccDNA to maintain a stable intranuclear pool [3]. Thus, the inhibition of HBV rcDNA production had a greater influence on the amounts of extracellular virions than the intranuclear cccDNA levels [29,30]. In our study, we hypothesize that the inhibition of HBV RNA production by the silver nanoparticles might in turn reduce the formation of rcDNA, and subsequently decrease the number of extracellular virions. However, because the inhibitory effects of silver nanoparticles are moderate (maximum 72.5% inhibition of HBV RNA), there might be still enough rcDNA to complement the cccDNA pool in the nucleus. This hypothesis would explain why the silver nanoparticles had little effect on the HBV cccDNA levels, but still needs further investigation.

Interaction between HBV DNA and silver nanoparticles

Silver nanoparticles have special properties, such as a larger active surface area and increased porosity, which facilitate their interaction with other small particles and molecules [31]. On this basis, we hypothesized that Ag10Ns might impede the transcription of viral RNA by binding to directly or interacting with HBV DNA, which serves as the template of RNA synthesis. Gel mobility shift assays were employed to assess binding potential. HBV dsDNA was treated with Ag10Ns at different molar ratios (DNA:Ag10Ns 1:50, 1:5, 1:0.5 and 1:0.05) or with a vehicle control and the complexes formed resolved by agarose gel electrophoresis (Figure 4A). All samples treated with Ag10Ns were found to exhibit 'shifting-up' effects, even at the 1:0.05 molar ratio, and the 1:50 sample was found to exhibit a significant tailing effect. This effect resulted from the substantial binding of silver

Figure 4. Interactions between HBV DNA and silver nanoparticles
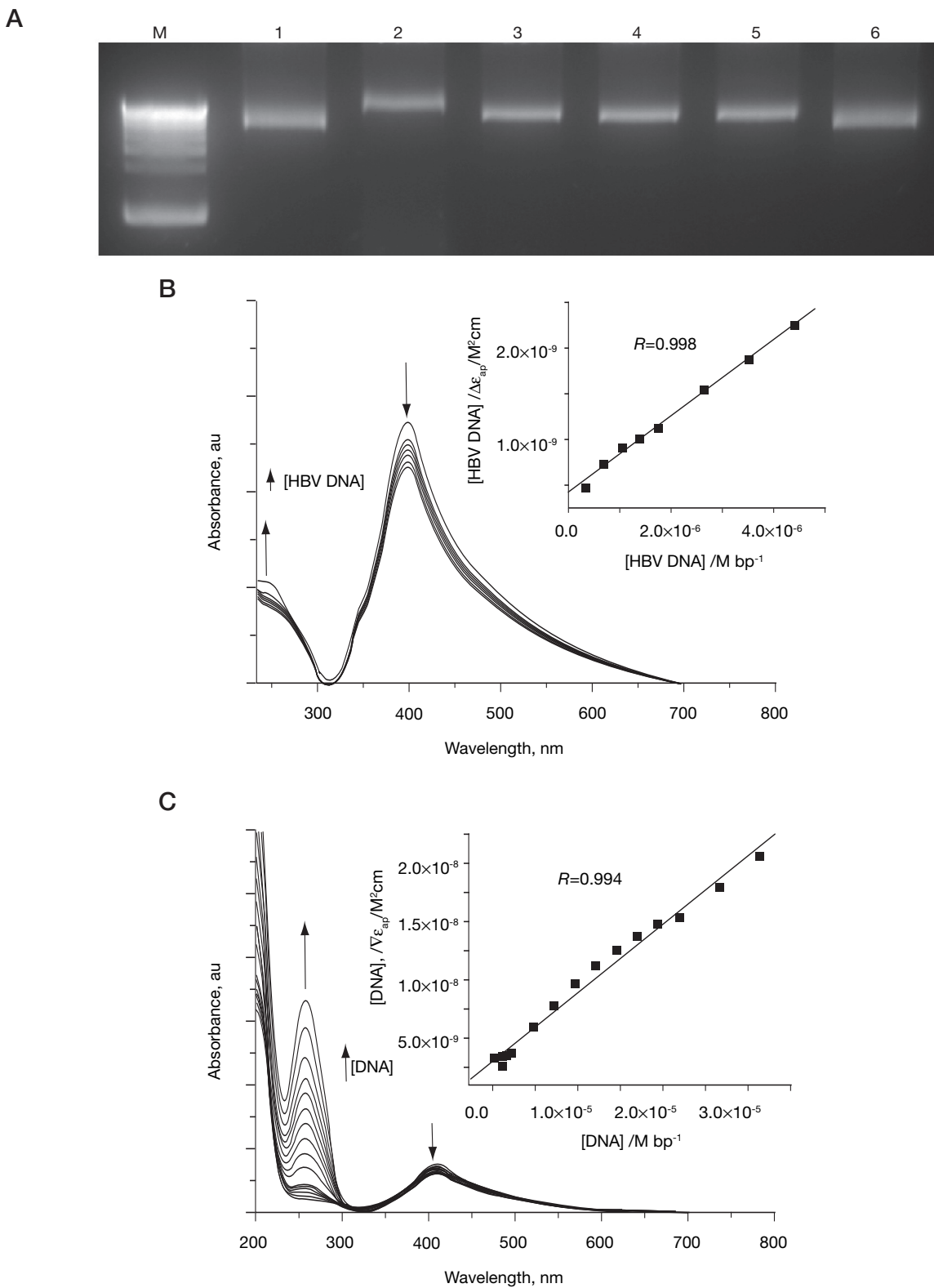
(A) Gel mobility shift assay of hepatitis B virus (HBV) double-stranded (ds) DNA and silver nanoparticles. M, Marker; (lane 1) HBV dsDNA (vehicle control); (lane 2) dsDNA:Ag10Ns 1:50; (lane 3) dsDNA:Ag10Ns 1:5; (lane 4) dsDNA:Ag10Ns 1:0.5; (lane 5) dsDNA:Ag10Ns 1:0.05; (lane 6) HBV dsDNA (vehicle control). Electronic spectra of Ag10Ns (50 µM) in TBS buffer with **(B)** increasing HBV DNA concentrations or **(C)** increasing calf thymus DNA concentrations at 298K. Inset: plots of [DNA]/$\Delta\varepsilon_{ap}$ versus [DNA].

Figure 5. Interaction between hepatitis B virus (HBV) viral particles and silver nanoparticles

A

B
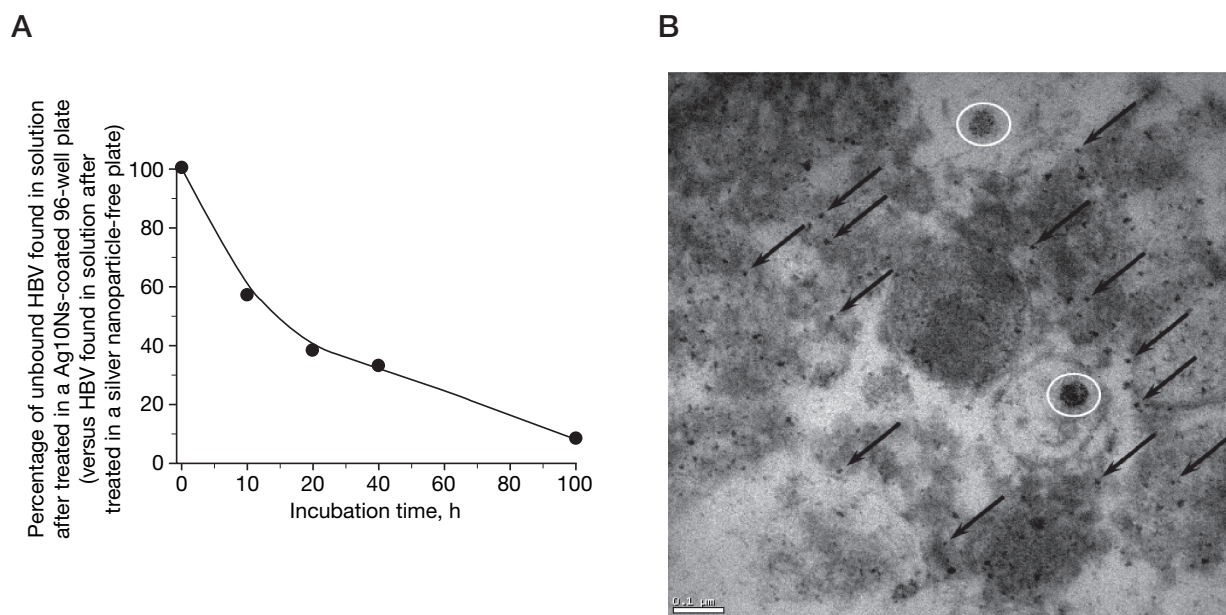
(A) Ag10Ns were coated on the surface of 96-well plates and serum samples of patients with chronic hepatitis B infection containing 1×10^7 HBV virions/ml were incubated in treated or untreated control wells for 0–60 min. At 10 min intervals, serum samples were collected to extract DNA and subjected to real-time PCR for HBV DNA quantification. **(B)** Transmission electron microscopy of ultrathin sections (50 nm) of Ag10Ns-treated (5 μM) HepAD38 cells. Selected HBV particles are marked by white circles and some silver nanoparticles are marked by black arrows.

nanoparticles to the HBV DNA, which augmented the size of DNA and increased the viscosity.

Binding constants were determined using a UV-vis absorption titration assay. The addition of aliquots of HBV DNA (0–100 μM) to a solution of Ag10Ns induced an isosbestic-spectral change with hyperchromicity of ~15% at its λ_{max} at 409 nm. The binding constant (K_b) of Ag10Ns towards the HBV DNA was found to be $(8.8 \pm 1.0) \times 10^5$ $dm^3 mol^{-1}$, which was determined from the plot of [HBV DNA]/$\Delta \varepsilon_{ap}$ versus [HBV DNA] (Figure 4B). Besides HBV DNA, we also found that Ag10Ns could bind to calf thymus DNA (ctDNA, Figure 4C) and the total RNA extracted from HepAD38 cells (Figure S4), with binding constants of $(1.5 \pm 0.3) \times 10^6$ and $(3.1 \pm 0.4) \times 10^5$ $dm^3 mol^{-1}$, respectively. Given the similar binding affinity to the ctDNA and RNA, we reason that the binding of Ag10Ns to the HBV DNA is non-specific and thus could contribute to the cytotoxic activity of silver nanoparticles at high concentrations.

Interaction between HBV viral particles and silver nanoparticles

Ag10Ns silver nanoparticles showed good binding affinity to HBV virions, as only 54% and 12% unbound viral particles (versus silver-nanoparticle-free control) were detected after incubation for 10 and 60 min,

respectively (Figure 5A). In addition, the distribution of Ag10Ns in HepAD38 cells was investigated using TEM. Ag10Ns was distributed mostly in the cell cytoplasm and the TEM image showed that several Ag10Ns bound to the HBV-like particles (Figure 5B). However, because the HepAD38 cell line is an HBV-integrated cellular model, whether this binding activity of silver nanoparticles can prevent HBV virions from entering into the host cells requires further investigation.

In summary, we report that silver nanoparticles possess high binding affinity for HBV dsDNA and extracellular virions, and could inhibit *in vitro* production of HBV RNA and extracellular virions.

Acknowledgements

Disclosure statement

The authors declare no conflict of interest.

Additional file

An additional file 'Supplementary material' containing Figures S1–S4 can be accessed via the Volume 13 Issue 2 contents page for *Antiviral Therapy*, which can be found at www.intmedpress.com (by clicking on 'Antiviral Therapy' then 'Journal PDFs').

References

1. Ganem D, Prince AM. Hepatitis B virus infection – natural history and clinical consequences. *N Engl J Med* 2004; **350**:1118–1129.

2. Lau GKK, Piratvisuth T, Luo KX, *et al*. Peginterferon alfa-2a, lamivudine, and the combination for HBeAg-positive chronic hepatitis B. *N Engl J Med* 2005; **352**:2682–2695.

3. Tuttleman JS, Pourcel C, Summers J. Formation of the pool of covalently closed circular viral-DNA in hepadnavirus-infected cells. *Cell* 1986; **47**:451–460.

4. Will H, Reiser W, Weimer T, *et al*. Replication strategy of human hepatitis B virus. *J Virol* 1987; **61**:904–911.

5. Summers J, Mason WS. Replication of the genome of a hepatitis-B-like virus by reverse transcription of an RNA intermediate. *Cell* 1982; **29**:403–415.

6. Lau GKK. Does treatment with interferon-based therapy improve the natural history of chronic hepatitis B infection? *J Hepatol* 2007; **46**:6–8.

7. Davis GL, Hoofnagle JH. Interferon in viral hepatitis: role in pathogenesis and treatment. *Hepatology* 1986; **6**:1038–1041.

8. Guidotti LG, Ishikawa T, Hobbs MV, Matzke B, Schreiber R, Chisari FV. Intracellular inactivation of the hepatitis B virus by cytotoxic T lymphocytes. *Immunity* 1996; **4**:25–36.

9. Perrillo RP, Schiff ER, Davis GL, *et al*. A randomized, controlled trial of interferon alfa-2b alone and after prednisone withdrawal for the treatment of chronic hepatitis B. *N Engl J Med* 1990; **323**:295–301.

10. Shaw T, Bartholomeusz A, Locarnini S. HBV drug resistance: mechanisms, detection and interpretation. *J Hepatol* 2006; **44**:593–606.

11. El-Sayed MA. Small is different: shape-, size-, and composition-dependent properties of some colloidal semiconductor nanocrystals. *Acc Chem Res* 2004; **37**:326–333.

12. Roduner E. Size matters: why nanomaterials are different. *Chem Soc Rev* 2006; **35**:583–592.

13. Merga G, Wilson R, Lynn G, Milosavljevic BH, Meisel D. Redox catalysis on 'naked' silver nanoparticles. *J Phy Chem C* 2007; **111**:12220–12226.

14. Mandal S, Phadtare S, Sastry M. Interfacing biology with nanoparticles. *Curr Appl Phy* 2005; **5**:118–127

15. Vinogradov SV. Colloidal microgels in drug delivery applications. *Curr Pharm Design* 2006; **12**:4703–4712.

16. Lok CN, Ho CM, Chen R, *et al*. Proteomic analysis of the mode of antibacterial action of silver nanoparticles. *J Proteome Res* 2006; **5**:916–924.

17. Wright JB, Lam K, Hansen D, Burrell RE. Efficacy of topical silver against fungal burn wound pathogens. *Am J Infect Control* 1999; **27**:344–350.

18. Sun RWY, Chen R, Chung NPY, Ho CM, Lin CLS, Che CM. Silver nanoparticles fabricated in Hepes buffer exhibit cytoprotective activities toward HIV-1 infected cells. *Chem Commun* 2005:5059–5061.

19. Elechiguerra JL, Burt JL, Morones JR, *et al*. Interaction of silver nanoparticles with HIV-1. *J Nanobiotechnology* 2005; **3**:6.

20. Radloff C, Vaia RA, Brunton J, Bouwer GT, Ward VK. Metal nanoshell assembly on a virus bioscaffold. *Nano Lett* 2005; **5**:1187–1191.

21. Ladner SK, Otto MJ, Barker CS, *et al*. Inducible expression of human hepatitis B virus (HBV) in stably transfected hepatoblastoma cells: a novel system for screening potential inhibitors of HBV replication. *Antimicrob Agents Chemother* 1997; **41**:1715–1720.

22. Hui CK, Cheung WWW, Zhang HY, *et al*. Kinetics and risk of *de novo* hepatitis B infection in HBsAg-negative patients undergoing cytotoxic chemotherapy. *Gastroenterology* 2006; **131**:59–68.

23. Mosmann T. Rapid colorimetric assay for cellular growth and survival: application to proliferation and cytotoxicity assays. *J Immunol Methods* 1983; **65**:55–63.

24. Bowden S, Jackson K, Littlejohn M, Locarnini S. Quantification of HBV covalently closed circular DNA from liver tissue by real-time PCR. *Methods Mol Med* 2004; **95**:41–50.

25. Livak KJ, Schmittgen TD. Analysis of relative gene expression data using real-time quantitative PCR and the 2(-Delta Delta C(T)) method. *Methods* 2001; **25**:402–408.

26. Li CKL, Sun RWY, Kui SCF, Zhu N, Che CM. Anticancer cyclometalated $[Au^{III}_m(C{\wedge}N{\wedge}C)_mL]^{n+}$ compounds: synthesis and cytotoxic properties. *Chem Eur J* 2006; **12**:5253–5266.

27. Günther S, Li BC, Miska S, Krüger DH, Meisel H, Will H. A novel method for efficient amplification of whole hepatitis B virus genomes permits rapid functional analysis and reveals deletion mutants in immunosuppressed patients. *J Virol* 1995; **69**:5437–5444.

28. Wolfe A, Shimer GH, Meehan T. Polycyclic aromatic hydrocarbons physically intercalate into duplex regions of denatured DNA. *Biochemistry* 1987; **26**:6392–6396.

29. Cacciola I, Pollicino T, Squadrito G, *et al*. Quantification of intrahepatic hepatitis B virus (HBV) DNA in patients with chronic HBV infection. *Hepatology* 2000; **31**:507–512.

30. Sung JJY, Wong ML, Bowden S, *et al*. Intrahepatic hepatitis B virus covalently closed circular DNA can be a predictor of sustained response to therapy. *Gastroenterology* 2005; **128**:1890–1897.

31. Alt V, Bechert T, Steinrucke P, *et al*. An *in vitro* assessment of the antibacterial properties and cytotoxicity of nanoparticulate silver bone cement. *Biomaterials* 2004; **25**:4383–4391.